ISSN 1063-7842, Technical Physics, 2021, Vol. 66, No. 9, pp. 1049–1057. © Pleiades Publishing, Ltd., 2021.
ISSN 1063-7842, Technical Physics, 2021. © Pleiades Publishing, Ltd., 2021.
Russian Text © The Author(s), 2021, published in Zhurnal Tekhnicheskoi Fiziki, 2021, Vol. 91, No. 7, pp. 1139–1147.

Migration of γ/α Phase Boundaries As the Initial Stage of the Inverse α → γ Transformation upon Slow Heating of Fe–32 at % Ni Metastable Alloy

N. D. Zemtsova

Mikheev Institute of Metal Physics, Ural Branch, Russian Academy of Sciences, Yekaterinburg, 620990 Russia

e-mail: zemtsova@imp.uran.ru

Received December 14, 2020; revised January 15, 2021; accepted January 27, 2021

Abstract—During quenching of Fe–Ni metastable alloys with the invar composition from the austenite region, precipitating Fe_3Ni disperse particles are transformed into the α-martensite structure upon cooling of the alloy in liquid nitrogen. Under slow heating, the inverse α → γ transformation is initiated by the diffusion mechanism (and not the martensite mechanism as has been assumed until now) via migration of the γ/α phase boundaries, which is accompanied with coalescence of Fe_3Ni particles at these boundaries. The periodic distribution of lumped particles at the γ/α interfaces determines the periodic distribution of the mobility of various regions in phase boundaries. This leads to a change in the morphology of γ/α interfaces from the linear to serrate form in the course of diffusion-controlled evolution of the α → γ transformation.

DOI: 10.1134/S1063784221070161

INTRODUCTION

The results of analysis of phase and structural transformations in alloys of the Fe–Ni system have been reported in a large number of publications. However, even now, the interpretation of the mechanism of the inverse α → γ transformation reflects numerous contradictions in the interpretation of the results of investigations. This is primarily due to the lack of a reliably established equilibrium state diagram of the Fe–Ni. The state diagrams given in the reference and periodic literature differ drastically in their low-temperature region. Some of the state diagrams reflect the presence of only one ordered phase of $FeNi_3$, while others contain, apart from this phase, ordered phases FeNi ($L1_0$) and Fe_3Ni ($L1_2$) or only FeNi ($L1_0$). Detailed analysis of the state diagrams encountered in the literature is given in [1]. In our opinion, the most reliable is the phase diagram reported in [2] and shown in Fig. 1, which is not represented in reference books. This diagram contains regions corresponding to the formation of ordered phases Fe_3Ni ($L1_2$) and FeNi ($L1_0$). It is impossible to distinguish these phases in austenite and to identify their structure using transmission electron microscopy because atoms of the alloy components are neighbors in the Periodic Table of elements, and diffraction of X-rays and electrons proves to be ineffective for analyzing the phase separation because of their close scattering factors. For this reason, the observation of superstructure reflections on electron diffraction patterns of binary alloys in a wide range of compositions and after various thermal treatments is interpreted as the result of long-range concentration disordering in Ni_3Fe particles because of a strong deviation of compositions from stoichiometry. The diffuse scattering near Bragg sites of the reciprocal lattice and the formation of a tweed diffraction contrast on the structure images are interpreted as a consequence of the coherent coupling of particles with the matrix lattice.

A different opinion is also reflected in the literature. For example, the authors of [3, 4], who detected clearly manifested diffuse scattering at the sites and in the interstitial space of the reciprocal fcc lattice of the solid solution of metastable austenite of Fe–Ni alloys and the tweed diffraction contrast in the form of ripples [3] on electronic microphotographs, explained their results by a changed fine structure of austenite, i.e., the presence of fluctuation displacement waves due to the instability of the fcc lattice near the temperature of the beginning of the martensite transformation. This conclusion was based on the detected increase in the intensity and length of diffuse scattering regions during sample cooling. In addition, in analysis of the austenite structure of binary alloys with a nickel content in the range 30–90%, these authors observed a more intense tweed contrast on the images of the structure of alloys with a lower concentration of nickel, which were recorded at room temperatures. The lowest intensity was observed for the N50 alloy

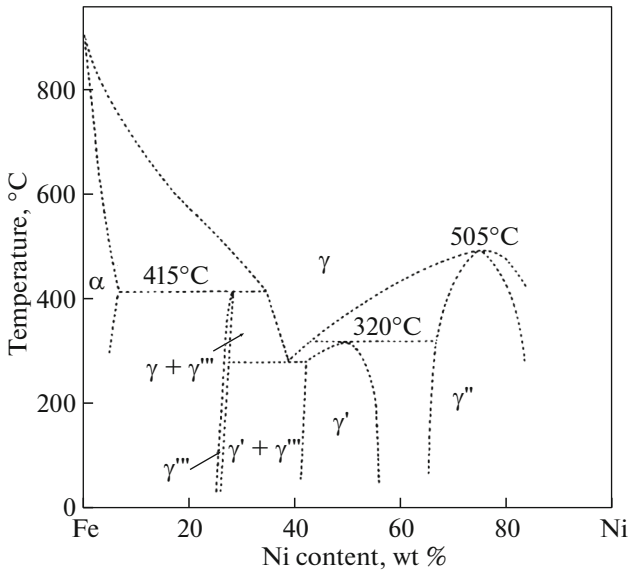

Fig. 1. Equilibrium phase diagram of Fe–Ni plotted based on structural methods of investigations and published in [2]; γ'' phase is Ni_3Fe ($L1_2$), γ' is FeNi ($L1_0$), and γ''' is Fe_3Ni ($L1_2$).

and for pure nickel, which confirms their conclusion about the existence of the premartensite effect precisely in metastable Fe–Ni alloys. The same experimental fact was reported in [5]. The authors of [6] stated that the tweed microstructure is not a premartensite effect, but gave no solid reason for this and only surmised the existence of oscillations of composition or order in the matrix of investigated alloys for explaining the observed diffraction effects.

The calculation of the total energy of Fe–Ni alloys experiencing the bcc and fcc transformation via Bain strain [7] revealed that the fcc and bcc lattices of the alloy under martensitic transformation preserve mechanical stability: these states correspond to energy minima separated by an energy barrier. The temperature dependence of the elastic moduli of the γ phase also does not confirm that there is loss of mechanical stability of the austenite lattice near the Ms point [8, 9].

Therefore, the literature data on the origin of the precipitating phase or its absence in Fe–Ni alloys with the invar composition, the tweed contrast on the images of the structure, and diffuse scattering on electron diffraction pattern are extremely contradictory.

Such different interpretations of the results of investigations would have been resolved if a reliable equilibrium state diagram of Fe–Ni could be obtained. Therefore, it is necessary to search for the ways of obtaining an equilibrium structure and the methods for its identification. The discontinuous reaction in the conditions of slow heating is known to lead to the formation of equilibrium phases for a given temperature [10]. In [11–15], the evolution of $\alpha \rightarrow \gamma$ transformation was detected for slow heating of metastable Fe–Ni-based alloys, which were in the initial $\alpha + \gamma$ state, via the migration of γ/α phase boundaries (this is equivalent to the discontinuous reaction of the $\alpha \rightarrow \gamma$ transformation; Fig. 2). Since this effect will be mainly used for obtaining an equilibrium structure, we consider the known experimental results of detection of the discontinuous reaction. The clumps of the discontinuous reaction are clearly seen in the microstructure of Fe–Ni–Ti alloys due to the separation of Ni_3Ti intermetallide (Fig. 2a) [11, 12]. In [13], a relief was detected along the phase boundary of the Fe–Ni binary alloy, which is not an indication of the martensitic mechanism of formation of reverted austenite because the formation of austenite from the α phase in accordance with any mechanism is accompanied by the formation of a relief on a preliminarily polished microsection due to the difference in the specific volumes of these phases (Fig. 2b). In [14], the realization of the $\alpha \rightarrow \gamma$ transformation governed by the discontinuous reaction mechanism in binary alloys was clearly demonstrated using interference microscopy (Fig. 2c). The clearly manifested curvature of the γ/α phase boundaries was demonstrated in [15, 16]. What, however, is the structure of regions of the discontinuous reaction in metastable Fe–Ni binary alloys? In this study, the results of investigation of the author in this field are considered. The initial state of the alloy is the two-phase state $\alpha + \gamma$, which is obtained by cooling of the initial austenite samples in liquid nitrogen.

1. MATERIAL AND EXPERIMENTAL TECHNIQUE

The Fe–32 at % Ni alloy was prepared from high-purity components. The carbon content did not exceed 0.01%. After homogenization at 1100°C for 48 h, the alloy was rapidly quenched in water. The resulting structure is characterized by X-ray diffractometry as austenitic. The sample of size 10 × 10 × 15 mm was prepared by electric-spark cutting. Cooling in liquid nitrogen and slow heating in air to room temperature led to the formation of about 80% of the α phase with a lenslike morphology. The sample placed into an evacuated ampule was then heated at a rate of 0.3°C/min to 400°C. The sample cooling to room temperature was carried out with the switched-off furnace. The sample was cut into two parts with an electric spark introducing the smallest distortions into the surface layer, and blanks for foils were cut from the middle part. After mechanical thinning of blanks with a small-grain polishing paper to a thickness of 0.2 mm, foils were prepared in an electrolyte based on orthophosphoric acid with addition of chromium anhydride and sulfuric acid at a voltage of 25 V.

The surface of the cut of the second part of the samples was polished with a small-grain polishing paper. To analyze the structure with a scanning electron microscope, the electropolishing and electroetching of the massive sample were carried out in the

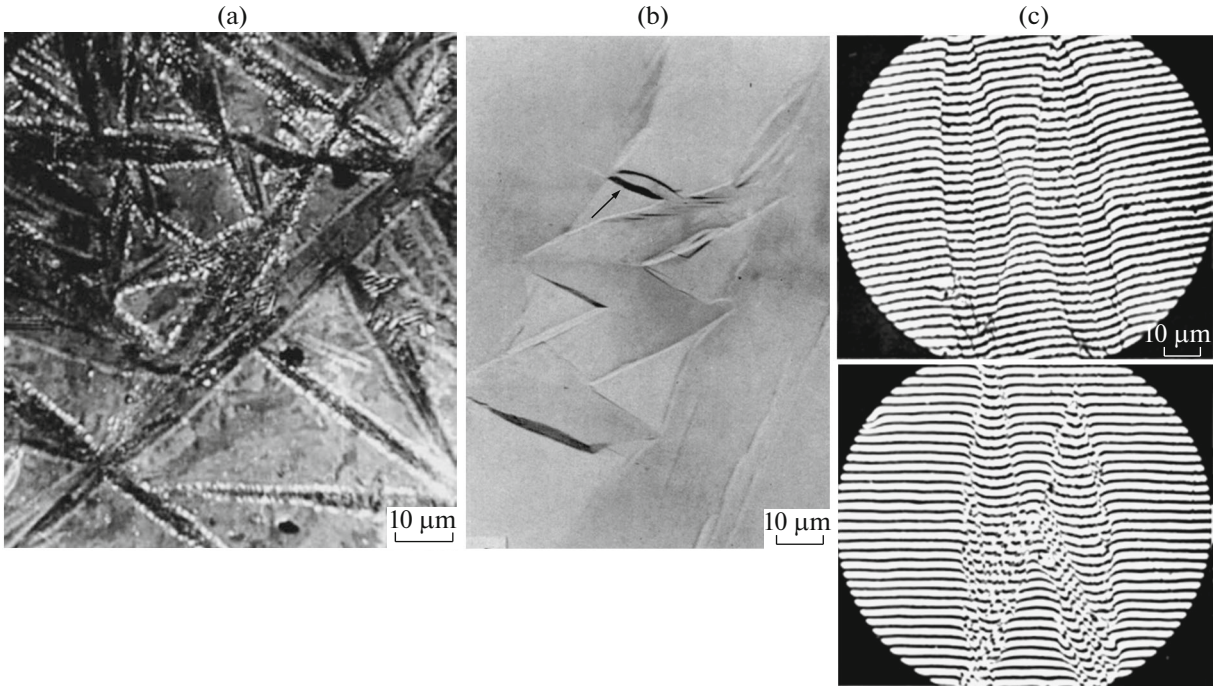

Fig. 2. Metallographically observed fringe of γ/α phase boundaries, which is formed during slow heating at the initial stage of evolution of the α → γ transformation via diffusion-controlled evolution of the discontinuous reaction (a) in the Fe–Ni–Ti alloy and (b, c) in Fe–Ni alloys of the invar composition recorded in (b) [5] and (c) [4].

electrolyte containing 90% glacial acetic acid and 10% chloric acid at a voltage of 100 V. The initial electrolyte temperature was 5°C. The obtaining of a sharp image of the structure in the scanning microscope requires deep etching ensuring a noticeable relief on the microsection surface. For this reason, electroetching lasted for at least 1 min. To reduce the sample heating in the zone of contact with the electrolyte, the sample was continuously jerked. Immediately after the electrical procedure, the samples were washed in alcohol or acetone to prevent oxidation of their surface.

The structure was analyzed at the Electron Microscopy Department of the Test Center of Nanotechnologies and Perspective Materials (Institute of Metal Physics, Ural Branch, Russian Academy of Sciences) on a Quanta-200 scanning electron microscope and on a JEM-200CX microscope under an applied voltage of 160 kV at room temperature.

2. RESULTS AND DISCUSSION

2.1. Experimental Proof of Precipitation of the Ordered Phase of Fe_3Ni in Residual Austenite

Figure 3a shows the structure of the alloy after its cooling in liquid nitrogen. The γ/α phase boundaries are crystallographically smooth without bends and protrusions.

The temperature of the beginning of the inverse α → γ transformation during heating at a rate of 0.3°C/min was determined using magnetometry [15]. It was found to be 310°C. Figure 3b shows the sample structure formed during heating to 400°C. With a large magnification, bending of the γ/α phase boundaries can be clearly seen (Figs. 3c, 3d). Consequently, the morphology of the γ/α phase boundaries has changed during their migration.

In Fig. 3c, the "ladder" in the central part of the figure is quite interesting. In our opinion, its origin becomes clear from Fig. 3e borrowed from [16]. This figure clearly demonstrates the teeth on the γ/α phase boundary, which cut deep into the bulk of the martensite lamella. In our figure, teeth (indicated by arrows), the ends of which form a ladder in the residual austenite structure located slightly higher than the martensite lamella and at a quite large angle, are also seen clearly. This means that the migration of the γ/α phase boundary occurs not completely, but for an individual periodically located region. Such a ladder structure could be observed on the plane intersecting the structure shown in Fig. 3e at an angle of 90°, the projection of which is shown by the red dashed line in the lower part of the figure.

In Fig. 3d, the sample structure is shown with a large magnification, which makes it possible to see individual particles located on slip traces of residual austenite (indicated by the arrow). Bulk compression of the residual austenite regions during the α → γ transformation, which leads to plastic deformation significantly changes the energy state of particles, ensuring coagulation of particles located on slip traces

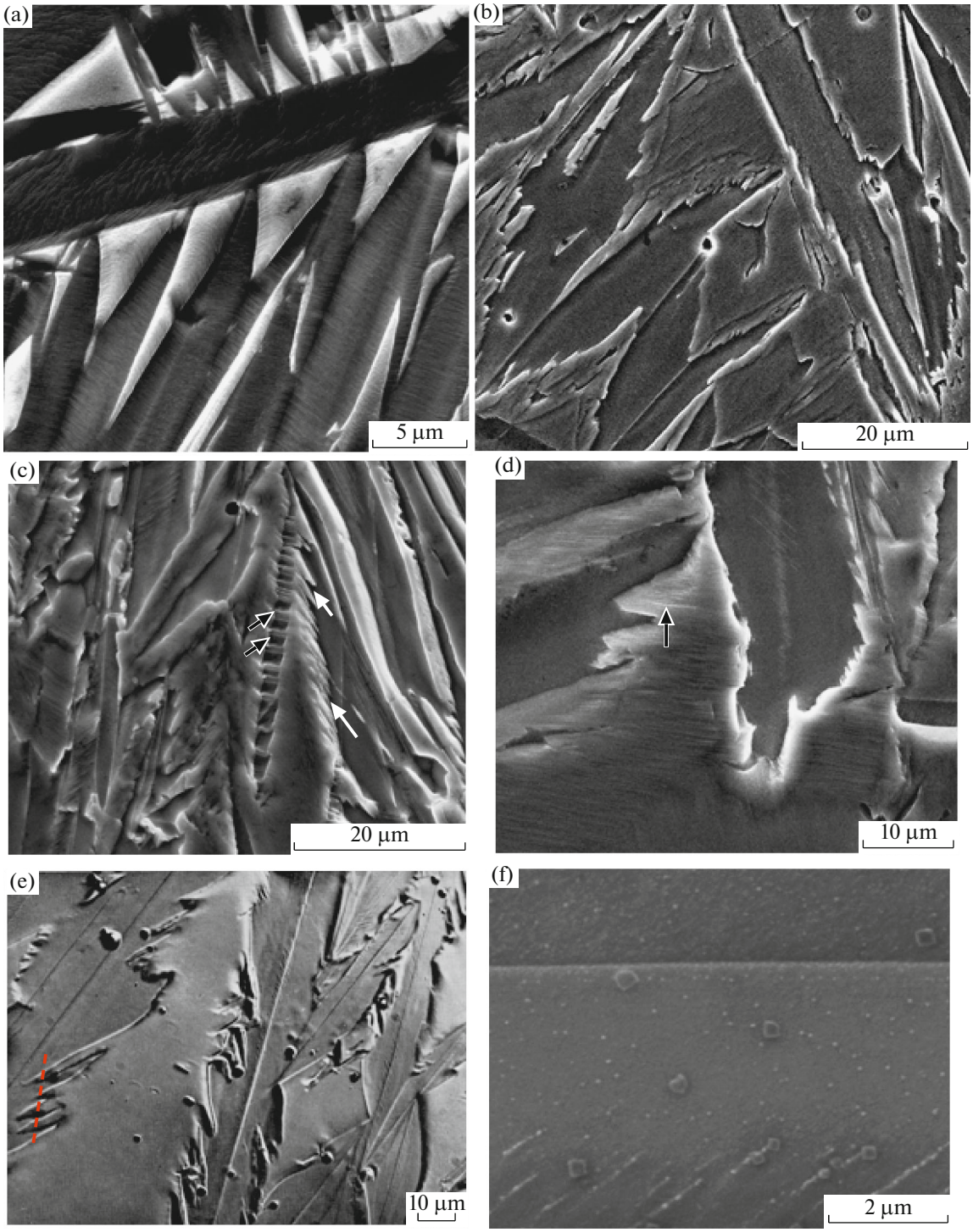

Fig. 3. SEM images of the structure of the Fe–32 at % Ni alloy: (a) after cooling in liquid nitrogen, γ/α phase boundaries are perfectly smooth; (b–d, f) after slow heating to 400°C, γ/α boundaries have acquires serrated morphology; (c) white arrows indicate the teeth forming a ladder, and black arrows indicate particles located at boundaries of the teeth; (d) particles located on the slip traces in residual austenite are indicated by arrow; (f) image of the boundary region at the γ/α interface, and coarse particles of the Fe_3Ni phase located in reverted austenite can be seen in the lower part of the panel; and (e) structure of the Fe–29 at % Ni alloy, borrowed from [16]; optical microphotograph; red dashed line in the lower part of the panel is the projection of the plane on which the ladder formed by the tips of the teeth could be seen.

during subsequent heating due to dissolution of particles in the surrounding matrix. Naturally, only α phase with a specific volume smaller than the specific volume of the austenite matrix will grow. According to the diagram of states given above, this may be an ordered phase containing mainly atoms of a smaller

radius. These are iron atoms, and the phase is $Fe_3Ni(L1_2)$.

Slip traces do not reach the γ/α phase boundary. Consequently, the region containing no slip traces has been formed during the migration of the γ/α boundary and is the region of reverted austenite formed at the initial stage of evolution of the reverse $\alpha \rightarrow \gamma$ transformation. This region is shown in Fig. 3f with a still stronger magnification. The phase boundary separates martensite depicted at the top of the figure (which appears darker because of stronger etching) from austenite (bottom part). In martensite, disperse particles of the phase separated during quenching of the alloy from the austenite region and converted into martensite during the $\gamma \rightarrow \alpha$ transformation upon the cooling of the alloy in liquid nitrogen can also be seen. In austenite, in the region of reverted austenite adjoining the interface (see Fig. 3f), much coarser particles of the precipitated phase as compared to particles in slip traces, as well as within the martensite lamella can be seen. Such coarse particles could be formed only as a result of discontinuous coagulation of particles of the precipitated phase during the evolution of the $\alpha \rightarrow \gamma$ transformation because the discontinuous coagulation is much more effective than the coagulation occurring in the bulk of the material [17–20].

Most often, the regions of discontinuous disintegration, as well as discontinuous coagulation regions, are characterized by the lamellar structure (alteration of the lamellar or fibrous structure of the precipitated phase with lamellas of the matrix depleted in doping element is observed).

In our case, not lamellas, but coarse square particles, of the precipitated phase are seen. Such a form of separation is possible in the case of precipitations with a lattice isomorphic to the matrix lattice. Moreover, even with such a form of precipitation, circular particles of the γ′ phase in 36NKhTYu and 36NKhT2Yu2 alloys are close to Ni_3Ti in their chemical composition [10]. The difference in the chemical compositions of precipitates and matrix led to a contrast appearing due to the difference in their structural factors [21]. In our case, precipitated particles even acquired a cubic shape, which was possible due to an insignificant difference in the lattice parameters of the matrix and precipitates [1, 2] and the coherent or quasi-coherent bond. The impossibility of visualization of particles of precipitated phase using electron microscopy indicates close values of the structural factors of the matric and precipitate, which is further confirmation of precipitation of the Fe_3Ni phase with a composition closest to that of the matrix. These particles can be visualized in martensite lamellas using transmission microscopy for a strong acting reflection of the α phase (Fig. 4).

The centers of a discontinuous reaction always have the two-phase structure. One of the phases is the precipitated phase. The other phase is the recrystallized matrix (reverted austenite in the given case). According to any diagram of states given in the literature, the reverted austenite nuclei must have an elevated content of nickel. This leads to the conclusion that the precipitated phase must be deplete in nickel in accordance with the law of conservation of matter. It can be concluded again that this phase can be only the ordered Fe_3Ni phase. The fluctuation-induced formation of a γ nucleus of the critical size with a nickel content of about 40% becomes possible precisely due to precipitation of Fe_3Ni particles with about 25 at % Ni.

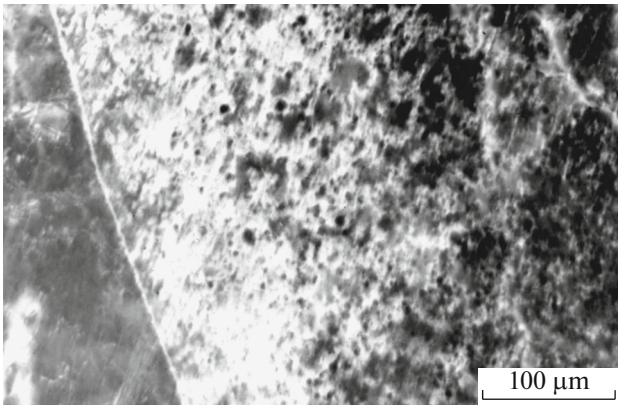

Fig. 4. TEM image of the alloy structure; black particles of the precipitated phase, which have passed to the martensite structure, can be seen.

Thus, we have demonstrated exclusively by logical comparison of our results with reliably established regularities of evolution of phase transformations that the precipitated phase in residual austenite during heating to 400°C is the Fe_3Ni phase. This conclusion is confirmed by experimental results obtained by many researchers who have detected the precipitation of the ordered phase in austenite of metastable Fe–Ni alloys with a Ni content from 27 to 36% [1] and serves as a sufficient additional substantiation for representing the phase diagram of Fe–Ni (see Fig. 1) as an equilibrium diagram.

2.2. Migration Mechanism of γ/α Boundaries

The necessary condition for discontinuous disintegration as well as discontinuous coagulation is the migration of phase boundaries. For its realization, an additional driving force apart from the chemical force is required. The role of such an additional force can be played by (i) the energy of the matrix crystal lattice distortions, which is induced by quenching as well as preliminary continuous decomposition and released during recrystallization, and (ii) the elevated surface energy of grain boundaries, which decreases during the recrystallization of the deformed material or collective recrystallization [22–25]. In this case, the migration of boundaries is the leading process in the

discontinuous reaction, and its boundary is convex. According to some data, an additional driving force can be the decrease in the interfacial surface energy of particles precipitated on the boundary [26, 27]. However, the authors of these publications present a diagram in which the discontinuous disintegration boundary has a convex shape.

According to the available results of thermodynamic calculations [28], the concave shape of a migrating boundary between particles should not lead to the evolution of discontinuous disintegration, but only to the formation of localized precipitations of a phase at grain boundaries.

However, these concepts refer to systems in which the primary process of nucleation and growth of discontinuous decomposition aggregates is the migration of a grain boundary. This, however, is not always the case: in the structure of Fe–Ni–Ti alloys, a concave shape of boundaries between the lamellas of the η phase have been detected experimentally [29, 30]. Such a form of discontinuous disintegration was observed in the matrix obtained by high-temperature annealing, which experiences collective recrystallization characterized by small-angle reorientation of coarse grains. A particle of the η phase precipitated at a grain boundary during subsequent annealing grows into one of the grains, distorting the grain lattice, which causes recrystallization due to the migration of the grain boundary through which the particle has grown. A center of the discontinuous disintegration appears. During the evolution of discontinuous disintegration, η-phase lamellas appear ahead of the transformation front and lead during their growth the moving boundary of the aggregate, remaining the leading phase. An analogous situation was noted in [31].

However, during the evolution of the reverse $\alpha \rightarrow \gamma$ transformation in the binary Fe–Ni alloy, which occurs during slow heating, the martensite crystal loses its stability at a certain temperature, which ensures an additional driving force for the evolution of a discontinuous coalescence of Fe_3Ni particles, accompanied with the formation of reverted austenite. This indicates that the discontinuous reaction boundary must be convex, and reverted austenite must be the leading phase.

The diffusion rate at a migrating boundary is approximately three times as high as the diffusion rate at a stationary boundary. Therefore, the evolution of the combined discontinuous reaction of coagulation of particles + formation of reverted austenite begins since the beginning of evolution of the $\alpha \rightarrow \gamma$ transformation. Owing to the accelerated diffusion along γ/α boundaries, the coalescence of Fe_3Ni particles arriving at a migrating boundary from the α phase during heating and subsequent annealing of the alloy occurs, which leads to their almost periodic arrangement on the boundaries. Since the lattice parameters of the phases in the entire range of compositions of Fe–Ni alloys differ insignificantly [2], the surface energy of a particle is low. Because of coalescence, the total surface energy of particles located at a phase boundary decreases. The particles that initially have a coherent or quasi-coherent bond with the structure of the phase boundary turn out to be more capable to growth. The γ/α boundaries can detach themselves from the particles and can move to the bulk of α lamellas containing disperse Fe_3Ni particles that must coagulate. The combined discontinuous reaction of the $\alpha \rightarrow \gamma$ conversion evolves. In the slow heating conditions, this reaction leads to the formation of equilibrium phases for the given temperature [10]: reverted austenite enriched by nickel, as well as coarse particles precipitated from the Fe_3Ni phase, must remain behind the migration front.

The regions of a boundary free of particles turn out to be in more favorable conditions for migration: these particles have a higher mobility than in the region of contact with a particle, where an additional driving force is required for overcoming elastic coherent stresses. For this reason, the γ/α boundary near a particle begins migrating later at a higher heating temperature. The migrating boundary in the central part between particles bulges, ensuring the formation of a "serrated" morphology of phase boundaries (see Fig. 3c).

Such a serrated morphology is enhanced during the evolution of the $\alpha \rightarrow \gamma$ transformation upon heating because the supply of nickel from the bulk of the martensite crystal is required for the propagation of the boundary (formation of reverted austenite). The middle part of a migrating region, which has penetrated more deeply into the bulk of the martensite crystal, is supplied with nickel more profoundly and is able to propagate further. The lengths of the nickel delivery path associated with bulk diffusion are different for regions of the boundary between particles and near them. This difference increases with temperature and leads to the clearly manifested serrated morphology of γ/α phase boundaries.

The redistribution of nickel atoms between the α and γ phases due to bulk diffusion of nickel leads to the formation of a nickel-depleted layer near the migrating boundary on the side of the α phase. In this case, in accordance with the equilibrium diagram of state for Fe–Ni, the temperature of the reverse $\alpha \rightarrow \gamma$ transformation in the layer gradually depleted in nickel increases; accordingly, the driving force of the reverse $\alpha \rightarrow \gamma$ transformation decreases. This depletion, which mainly occurs in the boundary regions close to coarse particles, reduces the additional driving force of the discontinuous reaction in such regions and facilitates the formation of the serrated morphology of γ/α phase boundaries.

Thus, the origin of the sawtooth shape of γ/α phase boundaries at the initial stage of the evolution of the

$\alpha \rightarrow \gamma$ transformation is determined by the following factors:

(i) the presence of excess phase particles in the structure of the α phase;

(ii) the coalescence of particles at phase boundaries, which leads to their periodic arrangement;

(iii) the difference in the magnitudes of the extra driving force required for the initiation of the discontinuous reaction near a particle and between particles;

(iv) the formation of a nickel-depleted region near a migrating boundary and the increase in the difference in the degrees of depletion near particles and between them because of the difference in the length of nickel delivery paths to these regions; and

(v) the proportional decrease in the driving force of the $\alpha \rightarrow \gamma$ transformation due to an increase in temperature A_S in different parts of the nickel-depleted region near a migrating boundary.

The evolution of the discontinuous reaction to a larger depth occurs for the middle part of the region, which is initially free of particles of the precipitated phase characterized by a higher mobility because the required number of nickel atoms is delivered for a longer time from the bulk of a martensite lamella only to this region. For this reason, the phase boundaries acquire serrated morphology. With the evolution of the combined discontinuous reaction of the $\alpha \rightarrow \gamma$ transformation, the delivery of nickel atoms due to bulk diffusion turns out to be insufficient for the formation of a nickel-enriched reverted austenite and the migration ability of phase boundaries decreases, as well as the boundary diffusion coefficient. This leads to the suppression of discontinuous coalescence of particles at phase boundaries. The latter are found to be coated with a thick network of Fe_3Ni particles that can be seen at the boundaries of "ladder steps" and are the boundaries of teeth of reverted austenite (see Fig. 3c; dark arrows indicate the boundaries of reverted austenite teeth).

The projection of the tips of the serrated structure of reverted austenite is clearly seen in Fig. 5. Thin "steps" of reverted austenite completely cross the martensite lamella, including the midrib. Particles of Fe_3Ni are clearly seen at their boundaries. Therefore, the combined discontinuous reaction of the $\alpha \rightarrow \gamma$ transformation cannot lead to the completion of the $\alpha \rightarrow \gamma$ transformation process. Its evolution turns out to be suppressed because, apart from the coagulation of particles, the formation of austenite enriched in nickel is required. The self-sustained $\alpha \rightarrow \gamma$ transformation can evolve only in the conditions of permanent supply of phase boundaries with nickel diffusing from the bulk of a martensite lamella. However, in the conditions of continuous increase in the diffusion path length of nickel atoms from the bulk of the α-phase lamella to γ/α boundaries, the length of each of the migrating segments decreases, and, with increasing time of its migration, the traversed path has the shape of a tooth on the plane, and the entire migrating boundary becomes serrated. The transformation intensity gradually decreases, and the process dies away with time.

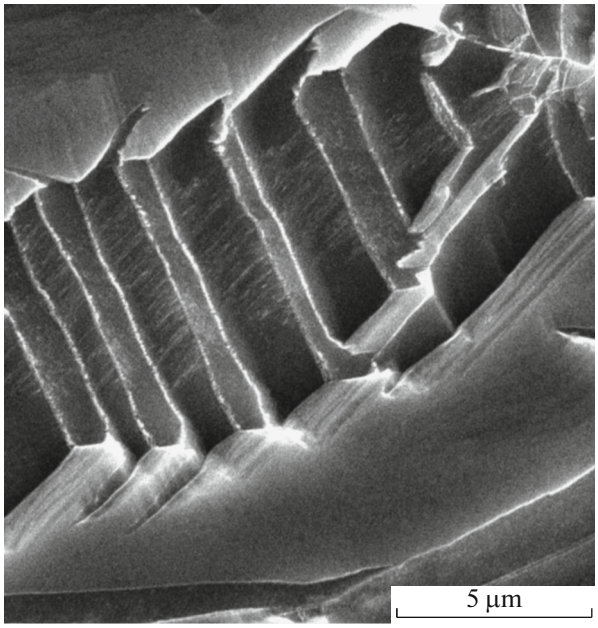

Fig. 5. Projection of the tips of the serrated structure of reverted austenite with particles of the Fe_3Ni phase at their boundaries.

The diffusion over γ/α phase boundaries, the coagulation of particles at these boundaries, and the supply of nickel atoms from the bulk of α-phase lamellas to the boundaries, which ensure the migration of phase boundaries in the conditions for combined discontinuous reaction of the $\alpha \rightarrow \gamma$ transformation, form a unique autocatalytic process.

In our opinion, we have proposed a quite convincing and experimentally substantiated conclusion concerning the type of the precipitated Fe_3Ni ($L1_2$) phase. All known experimental results including the decrease of the temperature corresponding to the beginning of the martensitic $\gamma \rightarrow \alpha$ transformation Ms after irradiation of a quenched alloy or after annealing at temperatures below 500°C (below the temperature of the Fe_3Ni phase disordering), the increase in the yield stress of austenite after such treatments, and the emergence of the paramagnetic peak in the resonance spectra of the nuclear γ resonance can be explained precisely by the precipitation of the Fe_3Ni disperse phase in austenite [1].

Thus, the rate of decrease in the free energy at the first stage of evolution of the $\alpha \rightarrow \gamma$ transformation is controlled by two processes: one occurring at the phase boundary and the other taking place within martensite lamellas.

This results in the emergence of serrated interfaces, which can easily be observed using the metallographic method of investigation as well. Sadovskii [32] wrote that, as one of the unsolved problems concerning the structural mechanism of the formation of austenite during heating, no one has even attempted to explain the origin of the serrated structure. In this study, not only has such an attempt been made, but its origin has been reliably established for metastable Fe–Ni-based alloys.

2.3. On the Tetragonality of Martensite in Fe–Ni Alloys

At present, the origin of tetragonality of iron–nickel martensite is not quite clear.

For the Fe–Ni–Ti alloys, the origin of tetragonality of freshly formed martensite obtained by cooling of austenite in liquid nitrogen has been demonstrated clearly and substantiated theoretically. These alloys cannot be quenched from the austenite high-temperature region with the conservation of the single-phase state. Austenite always contains disperse particles of the γ′ phase Ni_3Ti, which are coherently coupled with the austenite lattice and ordered according to the $L1_2$ type [33–35]. During cooling, these particles with the face-centered lattice and with the original austenite orientation are transformed into the martensite structure, preserving their coherence. Since the fcc lattice of particles is simultaneously a body-centered tetragonal lattice with a ratio of axes of $\sqrt{2}$, these particles with preserved coherence must induce the elastic tetragonal deformation of a body-centered α lattice. The superposition of the fields of static displacements from coherent particles, which are inherited by martensite from austenite, is experimentally manifested in the tetragonal distortion of the martensite crystal lattice.

The elastic strain of the particle material depends not only on the difference in the shapes and unit cell parameters of the γ′ phase and martensite, but also on the relation between the elastic moduli of these phases [7–9]. It is known that the degree of tetragonality of the martensite lattice in Fe–Ni–Ti alloys attains a value of $c/a = 1.04$ because of the presence of high-strength γ′ (Ni_3Ti) particles.

Copper particles inherited by martensite in Fe–Cu alloys are not effective shear centers in martensite and do not produce tetragonality [35]. In contrast to particles of the γ′ phase, these particles weakly affect the characteristics of the martensitic transformation because they are characterized by much smaller values of elastic constants as compared to iron–nickel austenite.

The Fe_3Ni particles precipitated in austenite during quenching of Fe–Ni binary alloys of the invar composition are also transformed into the martensite structure during cooling in liquid nitrogen and preserve the coherent coupling with its lattice. The elastic modulus of the Fe_3Ni phase is larger than the elastic modulus of copper particles; for this reason, these particles preserve the coherence with the martensite lattice. The degree of tetragonality of martensite of Fe–Ni alloys is low (1.004) [36]. However, residual austenite in both Fe–Ni and Fe–Cu alloys is coherently coupled with the martensite lattice. For this reason, it is not quite convincing to try to attribute the tetragonality of martensite in Fe–Ni alloys exclusively to coherent stresses at γ/α phase boundaries, as was done in [36]. If this were true, tetragonal distortions of the martensite lattice would be detected in Fe–Cu alloys also.

The tetragonality of the martensite lattice in Fe–Ni alloys is further evidence of the correctness of the Fe–Ni phase diagram shown in Fig. 1 and reported in [2], indicating the validity of the theoretical calculation of the stability of bcc and fcc phases to martensitic transformations in fcc and bcc, respectively. However, the lattices with tetragonal distortion of bcc and fcc structures turn out to be unstable to martensitic transformations [12]. The confirmed precipitation of the Fe_3Ni phase during quenching of austenite of metastable Fe–Ni alloys and the preservation of these precipitates in α-phase lamellas in the course of the $\gamma \rightarrow \alpha$ transformation introduce tetragonal distortions into fcc and bcc lattices of metastable Fe–Ni alloys, thus indicating the absence of formation of the premartensite state in metastable Fe–Ni alloys during cooling.

CONCLUSIONS

1. The precipitation of the Fe_3Ni phase in austenite of Fe–Ni binary alloys of the invar composition has been proved experimentally.

2. The correctness of the Fe–Ni phase diagram shown in Fig. 1 and published in [2], but not present in the reference literature, has been substantiated experimentally.

3. It is shown that, at the initial stage, the $\alpha \rightarrow \gamma$ transformation evolves in accordance with the mechanism of combined discontinuous reaction via migration of γ/α phase boundaries. The diffusion-controlled mobility of this boundaries becomes possible due to coagulation of Fe_3Ni particles at γ/α boundaries and diffusion-controlled delivery of nickel atoms from the bulk of martensite lamellas to phase boundaries.

4. The controlling effect of two phase transformations on the rate of evolution of the $\alpha \rightarrow \gamma$ transformations (one occurring at the interface and the other within martensite lamellas) determines the serrated morphology of γ/α phase boundaries.

5. The tetragonality of the crystal lattice of carbon-free iron–nickel martensite is explained by the existence of Fe_3Ni particles coherently coupled with the lattice in binary Fe–Ni alloys of the invar composition.

FUNDING

This study was performed in the framework of state order no. AAAA-A18-118020190116-6 for the Institute of Metal Physics, Ural Branch, Russian Academy of Sciences (theme "Structure").

CONFLICT OF INTEREST

The author declares that she has no conflicts of interest.

REFERENCES

1. N. D. Zemtsova, Phys.-Usp. **61** (10), 1000 (2018). https://doi.org/10.3367/UFNe.2018.02.038298]
2. A. Chamberod, J. Laugier, and J. M. Penisson, J. Magn. Magn. Mater. **10** (2–3), 139 (1979).
3. Yu. D. Tyapkin, V. G. Pushin, R. R. Romanova, and N. N. Buinov, Phys. Met. Metallogr. **41** (5), 1040 (1976).
4. V. G. Pushin, V. V. Kondrat'ev, and V. N. Khachin, *Pre-Transition Effects and Martensitic Transformations* (Ural. Otd. Ross. Akad. Nauk, Ekaterinburg, 1998) [in Russian].
5. G. Hausch and H. Warlimont, Acta Metall. **21** (4), 401 (1979).
6. M. Robertson and C. M. Wayman, Philos. Mag. A **48** (4), 629 (1983).
7. D. A. Mirzaev, E. A. Kabliman, and A. A. Mirzoev, Phys. Met. Metallogr. **113** (8), 774 (2012). https://doi.org/10.1134/50031918X12080078
8. K. Salama and G. A. Alers, J. Appl. Phys. **39** (10), 4857 (1968).
9. V. A. Lobodyuk and E. I. Estrin, *Martensitic Transformations* (Cambridge Int. Sci., London, 2014).
10. V. F. Sukhovarov, *Intermittent Phase Segregation in Alloys* (Nauka, Novosibirsk, 1983) [in Russian].
11. N. D. Zemtsova and E. I. Starthenko, Phys. Met. Metallogr. **50** (3), 600 (1980).
12. N. D. Zemtsova and E. I. Anufrieva, Phys. Met. Metallogr. **104** (6), 571 (2007). https://doi.org/10.1134/S0031918X07120058
13. H. Keßler and W. Pitsch, Arch. Eisenhüttenw. **38** (4), 321 (1967).
14. S. Jana and C. M. Wayman, Trans. Met. Soc. AIME **239**, 1187 (1967).
15. N. D. Zemtsova, Tech. Phys. **59** (9), 1150 (2014). https://doi.org/10.1134/S1063784214080295
16. R. L. Patterson and C. V. Wayman, Acta Metall. **14** (3), 347 (1966).
17. A. D. Korotaev, L. S. Bushnev, A. T. Protasov, and A. N. Tyumentsev, Izv. Vyssh. Uchebn. Zaved., Fiz. **1**, 108 (1970).
18. I. D. Livingston and I. W. Cahn, Acta Metall. **22**, 495 (1974).
19. E. Hornbogen and G. Pottermann, Z. Metallkd. **59** (10), 814 (1968).
20. G. R. Speich, Trans. Metall. Soc. AIME **227** (3), 518 (1963).
21. M. Ashby and L. Brown, in *Direct Methods of Investigating Defects in Crystals* (Mir, Moscow, 1965), p. 109 [in Russian].
22. W. Gruhl and H. Kramer, Metall. **12**, 707 (1958).
23. C. S. Smith, Trans. ASM **45**, 533 (1953).
24. Yu. A. Skakov, K. V. Varli, and G. K. Milovzorov, Izv. Akad. Nauk SSSR, Ser. Fiz. **34**, 1570 (1970).
25. R. A. Fornelle and J. B. Clark, Met. Trans. **3**, 2757 (1972).
26. K. N. Tu and D. Turnbull, Acta Metall. **17**, 1263 (1969).
27. K. N. Tu, Met. Trans. **3**, 2769 (1972).
28. H. J. Aaronson and H. B. Aaron, Met. Trans. **3**, 2743 (1972).
29. N. D. Zemtsova and K. A. Malyshev, Fiz. Met. Metalloved. **37** (6), 1209 (1974).
30. N. D. Zemtsova and K. A. Malyshev, in *Structural Mechanism of Phase Transformations of Metals and Alloys*, Eds. by O. S. Ivanov and R. M. Sofronova (Nauka, Moscow, 1976), p. 138 [in Russian].
31. B. R. Clark and F. B. Pikering, J. Iron Steel Inst., London **205** (1), 70 (1967).
32. V. D. Sadovskii, in *Structural Mechanism of Phase Transformations of Metals and Alloys*, Eds. by O. S. Ivanov and R. M. Sofronova (Nauka, Moscow, 1976), p. 5 [in Russian].
33. L. P. Gun'ko and V. V. Kokorin, Dokl. Akad. Nauk SSSR **240** (1), 72 (1978).
34. L. P. Gun'ko, Yu. N. Koval', L. E. Kozlova, V. V. Kokorin, and I. A. Osipenko, Fiz. Met. Metalloved. **53** (2), 326 (1982).
35. V. V. Kokorin, *Martensitic Transformations in Inhomogeneous Solid Solutions* (Naukova Dumka, Kiev, 1987) [in Russian].
36. V. I. Bondar', V. E. Danil'chenko, and V. A. Okhrimenko, Phys. Met. Metallogr. **66** (1), 146 (1988).

Translated by N. Wadhwa